Some First Results from the UAVSAR Instrument

Cathleen Jones, Scott Hensley*, Kevin Wheeler*, Greg Sadowy*, Scott Shaffer*, Howard Zebker†, Tim Miller*, Brandon Heavey*, Ernie Chuang*, Roger Chao*, Ken Vines*, Kouji Nishimoto*, Jack Prater*, Bruce Carrico*, Neil Chamberlain*, Joanne Shimada*, Marc Simard*, Bruce Chapman*, Ron Muellerschoen*, Charles Le*, Thierry Michel*, Gary Hamilton*, David Robison*, Greg Neumann*, Robert Meyer*, Phil Smith*, Jim Granger*, Paul Rosen*, Dennis Flower* and Robert Smith‡*

* Jet Propulsion Laboratory, California Institute of Technology, 4800 Oak Grove Drive, Pasadena, CA 91109
Email: cathleen.jones@jpl.nasa.gov
†Stanford University, Palo Alto, CA 94305
‡Goddard Space Flight Center, Greenbelt, MD 20771

ABSTRACT

The UAVSAR instrument, which employs an L-band actively electronically scanned antenna, has begun collecting engineering and science data after nearly three years of development. The radar system design was motivated by solid Earth applications where repeat pass radar interferometry can be used to measure subtle deformation of the surface. However flexibility and extensibility to support other applications and different platforms were also major design drivers. By designing the radar to be housed in an external unpressurized pod, it has the potential to be readily ported to many platforms. Initial testing is being carried out with the NASA Gulfstream III aircraft, which has been modified to accommodate the radar pod and has been equipped with precision autopilot capability developed by NASA Dryden Flight Research Center, which allows control of the platform flight path to within a 10 m diameter tube on any specified trajectory necessary for repeat-pass radar interferometric applications. To maintain the required pointing for repeat-pass interferometric applications we have employed an actively scanned antenna steered using INU measurement data. This paper presents a brief overview of the radar instrument and some of the first imagery obtained from the system.

I. INTRODUCTION

Earth science research often requires crustal deformation measurements at a variety of time scales, from seconds to decades. To meet these needs, the NASA Solid Earth Science Working Group has recommended an observational program that includes both airborne and spaceborne capabilities. Since many geophysical processes, such as volcanic eruptions and earthquake events, occur quickly and require near-immediate response by scientists and disaster managers alike, the goal is to provide Earth deformation measurements on an hourly basis with global access. While this objective is best supported by a spaceborne high-orbit (e.g. geosynchronous) constellation of repeat-pass interferometric SAR satellites, the recommended first step in this observational program is a low-earth-orbit deformation satellite with a repeat period of roughly one week. The sub-orbital radar program enters the Earth Science Enterprise plan as a key supplemental capability delivering the short time baseline observations, and providing repeat-pass measurements at time scales much smaller than one week, potentially as short as twenty minutes.

Although satellites have been used for repeat-track interferometric (RTI) SAR mapping for close to 20 years, repeat-track interferometry is much more difficult to implement from an airborne platform, [3]. Aircraft motion compensation methods have until recently not been sufficiently accurate to recover cm-scale deformations, and existing radar systems were designed without the necessary controls on flight position and antenna pointing to support repeat-pass InSAR. In fact, several organizations have acquired experimental airborne RTI data, but these lack the capability to routinely acquire significant amounts of scientifically useful RTI data. The primary technical reasons for this state of affairs remain: 1) it is difficult to fly the same or nearly the same pass twice in the troposphere due to wind gusts, turbulence, etc.; and 2) it is difficult to maintain the same antenna pointing on repeated passes due to varying cross-winds that lead to varying yaw angles. The UAVSAR system is specifically designed to overcome these limitations and produce high-quality RTI maps routinely.

The UAVSAR project will also serve as a technology test bed. As a modular instrument with numerous plug-and-play components, it will be possible to test new technologies for airborne and spaceborne applications with relatively little difficulty. Joint experiments with other radar instruments, for example, radars flying in formation with an active link between platforms, can also be accommodated without redesign of the system. The modular design also supports antennas at other radar frequencies. In fact, a Ka-band single-pass radar interferometer for making high precision topographic maps of ice sheets is being developed based to a large extent on components of the UAVSAR L-band radar.

II. INSTRUMENT DESIGN

Making robust repeat-pass radar interferometric measurements (RPI) at L-band to measure both natural and anthropogenically induced deformation of the Earth's surface from

Fig. 1. *Modified NASA Gulfstream III in early flight tests with the UAVSAR pod attached to the underside of the aircraft. Photo courtesy of NASA Dryden Flight Research Center.*

an airborne platform presents difficulties not found in space-borne observations due to the above mentioned navigation and pointing constraints. The UAVSAR radar is designed from the beginning as a miniaturized polarimetric L-band radar for repeat-pass and single-pass interferometry with options for along-track interferometry and additional frequencies of operation. Based on the science objectives and the platform characteristics, the key parameters of the radar design are given in Table I.

The radar will be initially deployed on the NASA Gulfstream III aircraft with the potential to be ported to other aircraft such as the Predator or Global Hawk UAVs. Figure 1 shows the instrument pod attached to the underside of the NASA Gulfstream III during early flight testing of the aircraft modifications. Key measurements the system has been designed to make in support of various NASA science programs include:

- Precision crustal deformation for monitoring earthquakes both during and after a seismic event, for monitoring volcanic activity and for monitoring human-induced surface change such as subsidence induced by oil or water withdrawal, or other displacements of the surface from human activities.
- Polarimetric interferometry, which can provide measurements of forest structure and sub-canopy topography.
- Polarimetric tomography, mapping in detail the vertical structure of a vegetated area.

Robust repeat-pass radar interferometric measurement needs impose two observational constraints on the UAVSAR radar and system. First, it is necessary that on repeat observations the aircraft fly within a specified distance of its previous flight trajectory. UAVSAR has a science-derived requirement for flight track repeatability of 10 m, hence NASA Dryden has modified the NASA Gulfstream III to include a Precision Autopilot capability [2] to control aircraft position. The precision autopilot uses input from the real-time DGPS (discussed in Section II-B) to generate signals that are used to drive the aircraft's ILS landing system. Early flight tests indicate that this requirement will be met. Secondly, it is also essential that the antenna look directions are identical within a fraction of the beamwidth. Because the wind can be substantially different at different times, even if the platform is capable of accurately repeating the desired track, the yaw angle of the aircraft can vary widely on different tracks due to different wind conditions aloft. UAVSAR thus employs an electronically steered flush mounted antenna that is pointed in the desired direction based on real-time attitude angle measurements.

TABLE I
RADAR PARAMETERS

Parameter	Value
Frequency	1.26 GHz (.2379 m)
Bandwidth	80 MHz
Pulse Duration	5-50 μs
Polarization	Quad Polarization
Range Swath	16 km
Look Angle Range	$25^\circ - 65^\circ$
Transmit Power	3.1 kW
Antenna Size	0.5m $\times$ 1.6 m
Operating Altitude Range	2000-18000 m
Ground Speed Range	100-250 m/s

Figure 2 shows a block diagram of the UAVSAR radar. After a brief overview of the block diagram each of the subsystems is discussed in further detail. The radar has been designed to minimize the number of interfaces with the aircraft for improved portability. The aircraft provides 28 V DC power to the radar via the Power Distribution Unit (PDU), which is also responsible for maintaining the thermal environment in the pod, and the radar provides its real-time DGPS position data to the aircraft for use by the Precision Autopilot. Waypoints for the desired flight paths are generated prior to flight by the Flight Planning Subsystem (FPS) and loaded into the Precision Autopilot and into the radar's Automatic Radar Controller (ARC) along with radar command information for each waypoint. The ARC is the main control computer for the radar and controls all major functions of the radar during flight. It is designed to operate in a fully autonomous mode or to accept commands from the Radar Operator Workstation (ROW) either through an ethernet connection on crewed platforms or through an Iridium modem for uncrewed platforms. The Control and Timing Unit (CTU) controls the timing of all the transmit and receive events in the radar timeline and thus interacts with many of the radar digital and radio frequency (RF) electronics. The active array antenna consists of 24 130 W L-band Transmit/Receive (TR) modules that feed 48 radiating elements within the 0.5 m by 1.5 m array. Figure 3 illustrates how the various electronic subsystems are arranged within the pod.

A. Digital Electronics Subsystem

The Digital Electronics Subsystem (DES) provides the overall timing and control signals for the radar as well as the telemetry and data acquisition functions. All the digital units are housed in a custom built VME card cage. Coordination and control of all the radar subsystems is through the master computer for the DES, the ARC. The ARC flight software controls the UAVSAR system for both attended and unattended

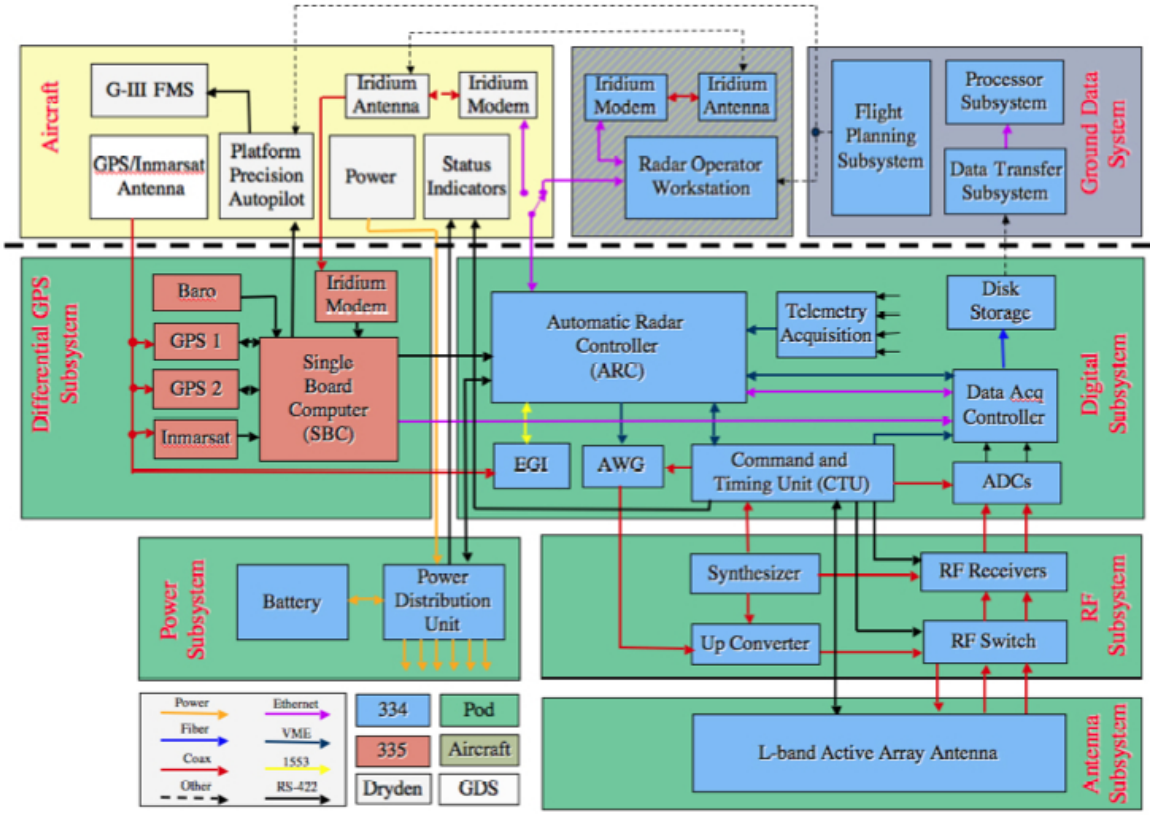

Fig. 2. *UAVSAR Radar Block Diagram, including aircraft, real-time differential GPS, and ground system interfaces. Color is used to code the various signal and control paths for the radar as indicated at the bottom left of the figure. The Iridium communication system can be used to communicate with the radar and GPS systems while in flight.*

flight operations. In many respects the ARC flight software must perform duties normally associated with spaceflight missions. This includes the ability to collect science data without operator intervention and to perform fault monitoring and recovery to minimize loss of mission objectives during flight. The ARC flight software utilizes the Wind River vxWorks operating system, a preemptive hard real-time kernel used by many flight projects at JPL. In addition to commanding the radar timing unit during science data collection, the ARC flight software handles the Embedded GPS/INU telemetry collection, tracks the aircraft flight path, performs electronic beam steering calculations, updates attenuation parameters and monitors temperatures inside the pod.

Precision timing of the pulse generation, ADC operation and antenna commanding are essential for proper radar operation. As the UAVSAR radar can operate in a number of complex modes including multi-polarization, multi-frequency and multi-antenna modes of operation, the CTU unit which controls all the precision timing was custom built at JPL using a Xilinx FPGA. The CTU provides receiver gains to the Radio Frequency Electronics System (RFES) based on commands sent from the ARC and provides a receiver protect signal to shut off the sensitive radar receivers during pulse transmission. Additionally, the CTU generates all the radar timing signals for the Arbitrary Waveform Generator (AWG), antenna, radar receivers and the data acquisition. All key radar events are time tagged by the CTU and recorded in the data header for subsequent processing.

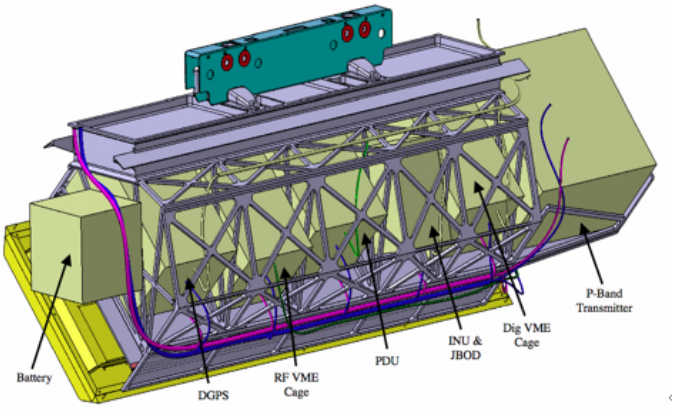

Fig. 3. *Diagram showing the location of the various electronic packages within the pod.*

After the returned data is digitized and possibly data compressed in the ADC board, it is buffered in the Data Acquisition Controller (DAC) along with an ancillary header and time tag data from the ARC and CTU. Information embedded in the header includes radar command parameters (e.g. PRF, gains, starting range, etc.), navigation data (e.g. position, velocity, attitude angles, etc.), time tags (both radar and GPS) and various data identification information. Raw signal and header data, as well as other ancillary files including GPS raw data file, data from the INU and a flight log file are stored onto

a disk array called a JBOD (just a bunch of discs). The SANBric JBOD is a hermetically sealed commercial off-the-shelf storage device with a capacity of 1.8 TB manufactured by Vmetro.

B. Navigation Subsystem

Repeat-pass radar interferometry requires highly accurate ephemeris and attitude information in real-time for flight path control, steering the electronic scanned antenna and for post processing of the SAR image data. UAVSAR's navigation subsystem consists of a real-time differential GPS and a commercial off-the-shelf INU. The real-time DGPS is a custom box developed by JPL that is a blend of commercial off-the-shelf components in a customized housing coupled with specialized software hosted on a single board computer. Data from NavCom and Ashtech (Magellan) GPS Receivers are blended with real-time correction data, broadcast via Inmarsat and Iridium satellite networks. While standard GPS position accuracy is 5-10 m, the UAVSAR DGPS uses correction information and JPL's Real-Time GIPSY software to achieve sub-meter precision. Testing results have shown that the DGPS easily meets the 1 m real-time requirement. The INU is a Litton LN-251, which is an integrated INU/GPS system that provides high accuracy position, velocity and attitude data at a 50 Hz rate. Data from the DGPS and INU are blended post-flight in the ground data system to generate the position and attitude data used to process the SAR data.

C. RF Subsystem

The Radio Frequency Electronic Subsystem (RFES) consists of three custom built units by Artemis, Inc. that are housed in a custom VME cage. The frequency synthesizer provides a 10 MHz reference signal for frequency generation, supplies a local oscillator (LO) signal for the upconverter and receivers, and a timing signal for the AWG. Upconversion of the baseband AWG center frequency of 137.5 MHz to the desired transmit center frequency of 1257.5 MHz and routing of the signals to the antenna switch network or receivers, as appropriate, are done in the upconverter unit. Dual L-band receivers take the returned signal from the H and V polarization channels and translate the L-band echo data down to 45 MHz prior to injection into the ADCs.

D. Antenna Subsystem

The antenna subsystem consists of an electronically-scanned phased array which allows the beam to be scanned along track to compensate for any aircraft yaw that differs from pass to pass in interferometric measurement mode. The antenna is composed of 48 (12 along track, 4 across track) patch radiating elements that are fed by 24 transmit / receive modules. Each module feeds a pair of patches in a column of four with the outer patches being fed at level 10 dB below the power level of the inner patches. This taper provides the wide beamwidth in the cross-track direction that is required for a large measurement swath and also suppresses sidelobes that otherwise lead to multipath from the aircraft wing.

The patch array is implemented in six tiles of eight patches each. Each tile is composed of a radiating patch layer made from Rogers RT/Duroid 6002 material, a low dielectric layer made from Astroquartz honeycomb and a stripline divider layer also made from RT/Duroid 6002. These materials were chosen for their RF performance and their excellent mechanical and electrical stability over temperature. Each patch is symmetrical and has orthogonal balanced feed points so that V and H polarization can be transmitted and received with good polarization purity. The stripline layer contains feed networks for both polarizations, including edge couplers to provide the 10 dB taper and 180 degree hybrids to provide balanced patch feeds.

The six radiating tiles are bonded to an aluminum honeycomb structure with their RF connectors protruding through holes in the structure. The rear side of the aluminum honeycomb panel carries all of the active electronics including TR modules, the Energy Storage Subsystem (ESS), RF manifolds, an Antenna Switch Network (ASN), TR and Antenna switch network Controller (TRAC) and DC/DC converters.

The TR modules (produced by REMEC Defense and Space) each contain a transmitter supplying approximately 130 W, and two receivers. All three channels have controllable phase and the receiver channels also have controllable gain. A calibrated phase and amplitude lookup table is loaded into each module prior to each data take. During the data take, the ARC uses information from the INU to continuously command the beam to be perpendicular to the current flight track. Upon receiving a steering command, each module loads the calibrated phase values for that particular steering direction into its phase shifters and programmable attenuators. The calibrated lookup table compensates for feed path length errors due to a module's position in the array and the measured temperature variation of that particular module, generating a nearly ideal aperture distribution for the desired scan angle.

The RF signals are distributed to and combined from the TR modules using stripline corporate networks implemented in three 9-layer RT/Duroid 6002 manifold boards. The upper and lower antenna halves have separate networks and there are separate networks for transmit, receive H, receive V, and calibration yielding a total of eight 12-way networks. All eight networks connect to the antenna switch network which connects the two receiver outputs to the H and V receivers of the full antenna or to the upper or lower halves of the antenna for either H or V. The ASN also allows loopback of calibration signals directly back to the receiver or through the TR modules.

The antenna subsystem is designed to receive unconditioned 28 V power from the aircraft and generate the voltages required for operation of its subassemblies. 9 V and -28 V power is generated by high-reliability COTS DC/DC converters, while the pulsed 31 V power required for the transmitters is supplied by six Energy Storage Subsystems. The ESS is a custom DC/DC converter with substantial charge storage and very low series resistance. This allows it to supply pulses of greater than 50 A with little voltage sag, minimizing

transmitter power droop over the pulse.

E. Power Distribution Unit

By electing to have a pod based radar sensor in an unpressurized pod to facilitate future transition to other platforms, the sensor design incurred a more complicated thermal control scenario. The power distribution unit is a custom JPL design that includes a Complex Programmable Logic Device (CPLD) for the thermal control algorithm, as well as provisions for taking the aircraft 28 V DC power and distributing to the various electronic subsystems. Temperature control for active array and radar electronics is accomplished using a combination of heaters and louvers that control the amount of air flowing through the cooling ducts.

F. Ground Data Subsystem

Repeat-pass airborne radar interferometry requires sophisticated processing algorithms to generate the desired deformation and associated science data products. The UAVSAR Ground Data System (GDS) consists of the hardware and software necessary to process and archive UAVSAR raw science data and the derived science products.

1) Image Formation, Interferometric and Science Processing: Generation of image and science data products follows motion processing. After the motion processing step is completed for a repeat-pass pair of images, a subsequent motion alignment algorithm is employed to determine proper processing parameters for the science data so that the imagery will be co-aligned in both the along-track and cross-track directions. Also, a common coordinate system and reference path based on the two trajectories is selected. Data for both passes are then processed through the image formation processor to generate single look complex (SLC) imagery. If the ephemeris knowledge were perfect then the two images would be co-registered precisely. However, even with the best post processing of the DGPS data, the expected relative position accuracy between the two passes is on the order of 2-3 cm, an order of magnitude or more larger than the required accuracy to achieve the fraction of a pixel offset that is required for interferometric applications. To achieve improved alignment, the relative position data, called the baseline, is refined based on the SLC images themselves. Several methods exist for recovering residual motion. These differ in implementation and accuracy, however, the basic idea is to use the misregistration information between the SLC images to derive a baseline correction. After the residual baseline is estimated the improved ephemeris is used to reprocess the data. The procedure may be repeated until the two images are co-registered with sufficient accuracy.

An interferogram is formed by multiplying the complex value of a pixel in one image by the complex conjugate of the corresponding pixel in the second image of the interferometric pair. It is the phase of the complex value in the interferogram that contains the deformation signal. However, the interferometric phase measurement suffers from two complicating factors that must be addressed before the deformation signal can be extracted. First, the interferometric phase encodes not only the surface deformation signal, but also a measurement of the surface topography whenever the baseline is non-zero. By simulating an interferogram using a digital elevation model (DEM) of the scene, the topographic signature component of the interferometric phase can be predicted and removed. Also, the interferometric phase is only measured modulo 2π, which represents one half wavelength (12 cm) of surface deformation. Since the deformation signal can be many multiples of 2π, a two dimensional phase unwrapping procedure is applied to get an unambiguous deformation measurement. After geocoding data from multiple repeat-passes, they are combined to reduce thermal and atmospheric noise, or, if the data are collected from multiple vantages, we reconstruct the three dimensional deformation vector. A single interferometric measurement is only sensitive to deformation in the line-of-sight direction.

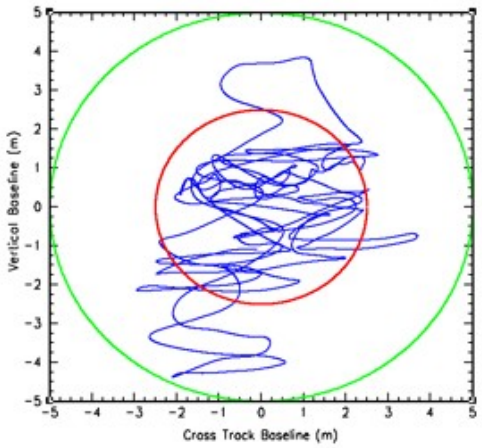

Fig. 4. *Repeat pass baseline for an 80 km flight line along the San Andreas fault south of San Francisco. The deviation of the two repeat tracks is shown, within a 10 m tube (red) and 20 m tube (green). The Precision Autopilot maintains the flight track within the desired 10 m tube over approximately 95% of the flight line.*

TABLE II
TEST FLIGHTS

Site	# flights	# lines
Long Valley, Ca.	2	4
Lost Hills, Ca.	2	8
Mt. Adams, Wa.	3	3
Mt. St. Helens, Wa.	3	23
Parkfield, Ca.	3	3
Rosamond, Ca.	10	75
Salton Sea, Ca.	2	4
San Franscisco Hayward Fault	4	22
San Franscisco San Andreas Fault	3	4
San Joaquin Valley, Ca.	2	2

III. FLIGHT TESTING OF THE INSTRUMENT

The UAVSAR flight testing schedule, which was compressed into about a year, was originally organized into three phases. The first phase is primarily dedicated to engineering checkout of the thermal control system, the radar instrument, and the Precision Autopilot Algorithm. These flights are designed to verify that the radar can collect good science data

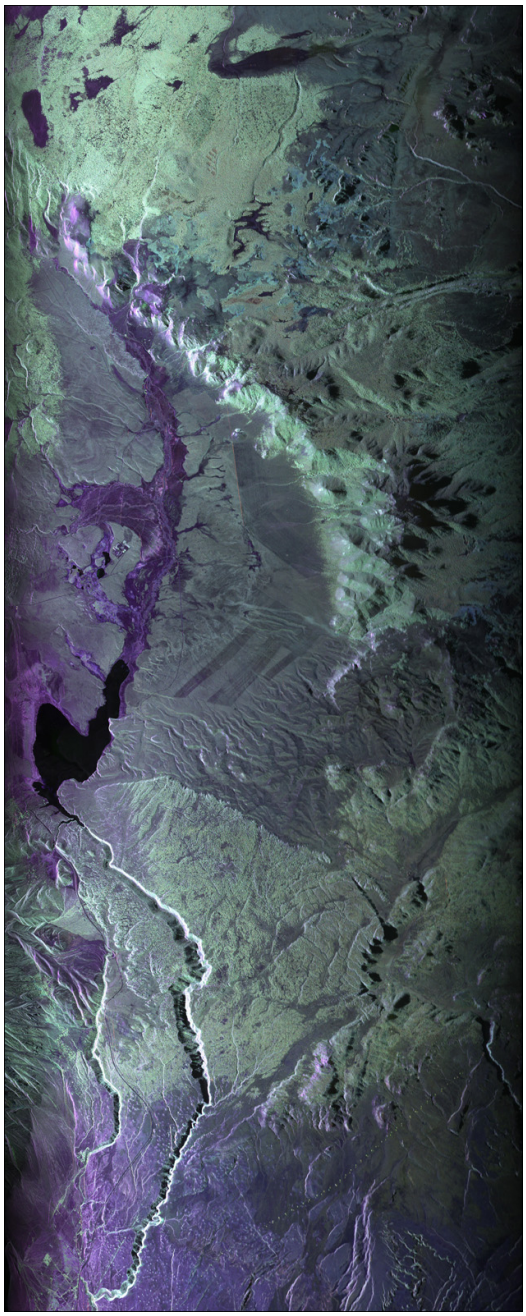

Fig. 5. *Polarimetric composite UAVSAR image of the Long Valley Caldera in northern California. The HH image layer is colored red, VV is colored blue and HV is colored green.*

in a variety of modes that cover the span of the adjustable radar parameters, under the full environmental range of its specified operating conditions. Particular emphasis is placed on verifying the stability and performance of the actively scanned array and of the automatic steering algorithms designed to maintain pointing within the required tolerances for repeat-pass interferometry. This phase is largely complete. Figure 4 shows the performance of the Precision Autopilot in repeating the platform's flight track on two different flights over the same area. In the diagram, the inner red tube represents the 10-m diameter tube about track and the outer green tube represents a 20-m diameter tube. The system, designed and implemented by Dryden FRC, maintains the repeat flight path within 5 m of the desired track for almost the entire data take. This performance is critical to the RPI capability of the UAVSAR platform.

The second phase of flight testing is designed to characterize and calibrate the radar instrument and to verify that performance is within requirements for the instrument. Characterization of the instrument entails establishing how much variation in phase or amplitude the radar undergoes as a function of temperature, antenna steering angle, mode or other adjustable radar parameters. Data for this purpose is generally collected over our corner refector array on the Rosamond dry lake bed or over the Central Valley of California. Much of the data has been acquired for these tests, although processing and calibration is ongoing. The final phase of testing, aimed at collecting science data, is devoted to repeat pass radar interferometric experiments over regions of scientific interest. Because of the tight flight schedule, both engineering checkout and the characterization and calibration data collection have been combined with science data collection flights to maximize the usage of the limited remaining flight hours. For the science data, test sites were chosen to look for surface deformation signatures in seismically active regions, volcanoes and at a site where anthropogenically induced surface deformation is occurring.

Limitations on the amount of fuel that the platform can carry and the allowed landing sites, which will be removed after the test program is complete, have constrained us to test flights over sites in California, Oregon, and Washington. We have collected approximately 2.5 TB of data during the test flights. Table II lists the sites, number of flights over each site, and number of lines collected at each site as of 5/15/2008. Typically, several sites will be imaged in a single four hour test flight. At least two flights suitable for RPI processing have been flown over each site originally selected. These are the San Andreas and Hayward fault lines in the San Francisco area; Parkfield, CA; the geothermal plants near the Salton Sea; and Mt. St. Helens in Washington state. Additional data has been collected over other sites, including the Lost Hills and Long Valley areas of California. We plan to continue flying one flight per week through the end of July 2008.

IV. FIRST IMAGES

UAVSAR collected its first image data on September 18, 2007 in a flight over the Rosamond Lake Bed in California (on a heading of 350 deg and at an altitude of 12500 m), where there is an array of trihedral corner reflectors used for calibration. Figure 5 shows a polarimetric composite image collected over the Long Valley Caldera in northern California. The radar was operated in its polarimetric mode and transmitted an 80 MHz bandwidth signal giving a range resolution of 1.66 m. The image covers an area 21 km wide by 90 km long. Data was received in the 12 to 8 bit Block Floating Point Quantization (BFPQ) compression mode. The center right of the image is Lake Crowley and to the right is the rim of the

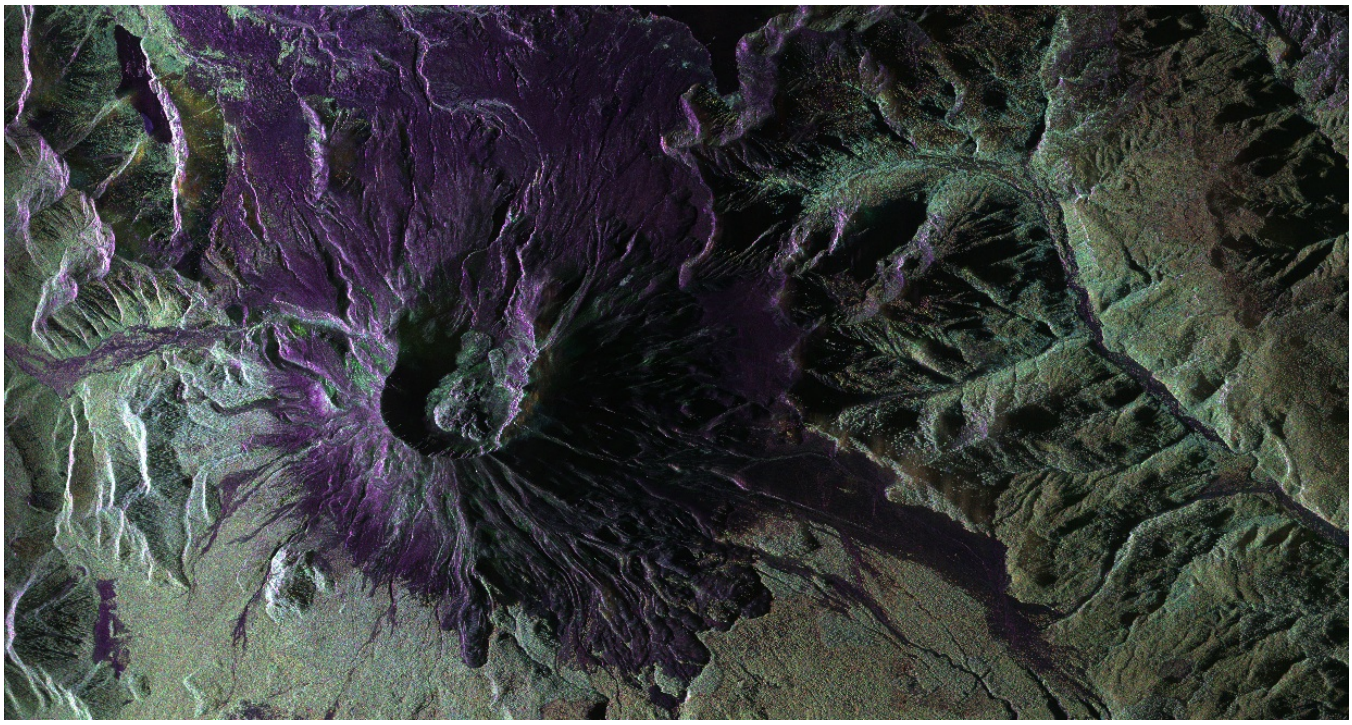

Fig. 6. *Polarimetric composite image of Mt. St. Helens. Within the caldera, the rising dome can be seen to the lower left. Two glaciers that are being pushed together as the dome rises are clearly visible to the upper right within the caldera.*

ancient caldera believed to last erupted about 800,000 years ago. In the lower right portion of the image is a series of dots that are power lines running through the scene.

The polarimetric image of the Mt. St. Helens volcano is shown in Figure 6. Although the data was collected when the peak was covered in snow, much detail is visible in the L-band radar imagery. The volcanic caldera dominates the image, with the dome visible to the lower left within the caldera. Two glaciers within the caldera, to the upper right of the dome, are being pushed together as the dome expands. The edge of Spirit Lake is at the upper center of the image and the tree line is visible in green. Repeat pass images of Mt. St. Helens will be used to measure the dome deformation and the glacier movement.

V. CONCLUSION

The UAVSAR instrument build is complete and the system currently undergoing flight test. This system will be the first civilian SAR to incorporate an electronically scanned array and is expected to provide a robust repeat-pass interferometric mapping capability to the science community. Initial flights and laboratory testing of the instrument indicate that it will meet its instrument and science requirements. The data from the flight tests will provide the first science data from UAVSAR, producing surface deformation maps with increased temporal and spatial resolution compared with existing spaceborne sensors. With future upgrades, UAVSAR will be able to support the science community beyond solid Earth, cryosphere, and land cover applications. The UAVSAR website, [1], contains sample images and additional information on UAVSAR.

ACKNOWLEDGMENT

A number of organizations have been integral to the development of the UAVSAR system. We would especially like to thank NASA Dryden for their overall leadership in the aircraft modifications, installation of the pod and development of the Precision Autopilot capability; Total Aircraft Services for the pod design and G-III modifications; REMEC Defense and Space for the development and supplying of the L-band TR modules; and Artemis for the design and manufacture of the modules in the RF subsystem. This research was conducted at the Jet Propulsion Laboratory, California Institute of Technology, under contract with the National Aeronautics and Space Administration.

Reference herein to any specific commercial product, process, or service by trade name, trademark, manufacturer, or otherwise, does not constitute or imply its endorsement by the United States Government or the Jet Propulsion Laboratory, California Institute of Technology.

REFERENCES

[1] http://uavsar.jpl.nasa.gov.

[2] James Lee, Brian Strovers, and Victor Lin. C-20A/GIII Precision Autopilot development in support of NASAs UAVSAR program. In *Proceeding of the NASA Science Technology Conference 2007*, Greenbelt, Maryland, June 2007. NASA.

[3] P. A. Rosen, S. Hensley, I. R. Joughin, F. K. Li, S. N Madsen, E. Rodriquez, and R. M. Goldstein. Synthetic Aperture Radar Interferometry. *Proc. IEEE*, 88:333–382, 2000.